

Received August 2, 2019, accepted August 15, 2019, date of publication August 19, 2019, date of current version August 31, 2019.

Digital Object Identifier 10.1109/ACCESS.2019.2936237

1-D Electronic Beam-Steering Partially Reflective Surface Antenna

LU-YANG JI¹, PEI-YUAN QIN², (Member, IEEE), JIAN-YING LI¹, AND LIN-XI ZHANG¹

¹School of Electronics and Information, Northwestern Polytechnical University, Xi'an 710129, China

²Global Big Data Technologies Centre, University of Technology Sydney, Ultimo, NSW 2007, Australia

Corresponding author: Lu-Yang Ji (luyangji@nwpu.edu.cn).

This work was supported in part by the National Natural Science Foundation of China under Grant 61701411, and in part by the National Science Key Laboratory Foundation under Grant 614240205070817.

ABSTRACT A 1-D electronic beam-steering partially reflective surface (PRS) antenna using a new reconfigurable PRS unit cell is proposed in this paper. The proposed work addresses the challenge to achieve a large beam steering angle with small gain variation and a small number of active/lumped elements by using a reconfigurable PRS superstrate only. The PRS unit cell consists of two back-to-back T-shaped strips with one PIN diode inserted between them and a pair of trapezoid patches (a rectangular patch and a pair of triangle parasitic patches). Beam steering is achieved by controlling the different states of PIN diodes. Thanks to the trapezoid patches, the proposed unit cell can generate a larger phase difference between different states, thereby leading to a larger beam steering angle. Furthermore, due to the addition of more degrees of freedom in the proposed unit cell, the phase difference can be easily manipulated. Moreover, since the T-shaped strips in each unit cell is connected with adjacent ones, the biasing network is very simple without needing a large number of lumped elements and dc biasing lines. The beam steering property is analyzed by using phased array theory. An antenna prototype with a main beam direction towards 0° , -18° and 18° operating at 5.5 GHz in the H-plane is fabricated and measured. Good agreement between the predicted simulation and measurement results for the input reflection coefficients and radiation patterns is achieved, which validates the feasibility of the design. The measured realized gains are over 11 dBi for all states with a 0.8 dBi gain variation.

INDEX TERMS Partially reflective surface antenna, beam steering, pattern reconfigurable antenna.

I. INTRODUCTION

Partially reflective surface (PRS) antenna has been intensively investigated because it can easily realize high gain with simple structure [1], [2]. It usually employs a small antenna acting as the radiating source and a periodic reflective superstrate. When the distance between the source and superstrate is approximately half a wavelength, the resonance condition is achieved to enhance the gains [3], [4]. Moreover, PRS antenna can achieve wideband property when a multi-layer reflective surface or a modified ground plane structure is employed [5]–[8].

Beam steering property has attracted much attention owing to its capabilities to provide large coverage. Phased array theory is a classical approach for antennas to achieve rapid beam scan [9]–[11]. The beam steering is realized by properly tuning the phase of each array element. The disadvantages of

phased arrays, however, are their high costs due to the use of transceiver modules and transmission-line feeding networks.

In most cases, PRS antenna can only generate a directive broadside beam. However, it has the potential to realize beam steering with relatively low cost when a variable phase distribution is employed on the upper PRS structure or on the ground plane. The design in [12] utilizes a phase-varying metasurface to control the reflection phase of the PRS and a passive beam steering at 9.5 GHz is achieved by changing the PRS dimensions. In [13], the proposed antenna can realize a beam scan up to 40° by mechanically rotating the metasurface in order to vary the PRS inductance. It should be noted that the antennas in [12] and [13] may not be suitable for applications where electronic reconfiguration is needed to achieve very fast beam steering. Recently, research efforts have been devoted to electronic reconfiguration of PRS antennas using active elements, such as PIN diodes and varactors [14]–[17]. The PRS antenna in [14] can realize frequency reconfiguration in the range of 1.9–2.31 GHz by

The associate editor coordinating the review of this article and approving it for publication was Shah Nawaz Burokur.

tuning the varactors on the upper LC-resonant metasurface. A beam steering PRS antenna is presented in [15], which can realize a beam scanning range of $\pm 7^\circ$ with respect to the broadside by using 144 varactor diodes to change the capacitance of the PRS structure. The beam of the PRS antenna in [16] can be tilted to $\pm 28^\circ$ by controlling the varactor diodes integrated with the unit cells of the PRS. In [17], the authors proposed a beam steering PRS antenna by employing a reconfigurable superstrate in combination with a phased array source. The entire reconfigurable PRS superstrate is divided into two parts integrated with 72 PIN diodes and 52 inductors. A $\pm 5^\circ$ beam steering angle is achieved by using the PRS superstrate only. Its gain variation is over 2.5 dBi. Furthermore, phase-modulated unit cells can be employed on the ground plane as high impedance surface (HIS) [18], [19]. By varying the states of the reconfigurable HIS unit cells, the PRS antenna in [18] can realize a continuous beam steering from 9° to 30° at 5.6 GHz. In [20]–[22], 2-D (azimuth and elevation) beam steering PRS antennas are achieved. By controlling the varactors on the unit cells, the design in [20] can work on three scanning modes and generate a pencil beam at eight azimuthal directions. However, it is very challenging to achieve -10 dB impedance matching for all the 9 states. The PRS antenna in [21] and [22] can achieve $\pm 10^\circ$ and $\pm 22^\circ$ 2-D beam steering at 5.5GHz with 144 and 72 PIN diodes, respectively.

Whilst the progress in the design of beam steering PRS antenna has been encouraging, major advances are required in the following areas. The first one is to achieve larger beam steering angles, preferably by using a reconfigurable PRS only to maintain system simplicity. Since the beam steering angle increases with the phase difference which is generated by different phases on different PRS parts, new method is needed to enlarge the phase variation range across the PRS. It is worth noting that although the beam steering angle can be further improved by using a phased array source [17], it compromised the advantages of PRS antenna since complicated reconfigurable phase network is needed. Large gain variation of the reconfigurable PRS antenna is the second issue. It is related to the difference of the reflection magnitudes between different parts of the PRS. This should be kept as small as possible. The third one is to reduce the number of active elements used in order to reduce the costs and losses, and to simplify the biasing network. Most designs reported to date use a large number of active/lumped elements. In short, a reconfigurable PRS antenna with a large beam steering range, a small gain variation and reduced active/lumped elements is highly desired.

This paper proposes an electronic beam steering PRS antenna addressing the above challenges by using a new reconfigurable PRS structure. The unit cell of the PRS consists of two back-to-back T-shaped strips in the center, coupled with a pair of trapezoid patches (a rectangular patch and a pair of triangle parasitic patches). Compared with other unit cells, the phase difference in the proposed structure can be made larger which is analyzed by phased array theory,

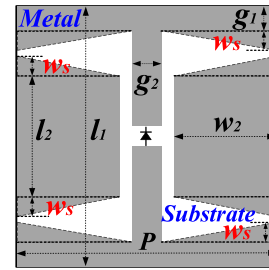


FIGURE 1. Schematic of the proposed unit.

TABLE 1. Dimensions of the proposed unit.

l_1	l_2	g_1	g_2
20 mm	10 mm	1.5 mm	3 mm

and it can be easily manipulated because more degrees of freedom have been added in the unit cell. Moreover, the reflection magnitudes between different states of the PRS are very close, leading to a small gain variation range. Furthermore, due to the specific structure of the proposed unit cell, only 36 PIN diodes are used, which is half of those in [17]. An antenna prototype is fabricated to verify the design concept. The center operating frequency of the proposed antenna is 5.5 GHz. The reconfigurable PRS can lead to a beam steering angle of $\pm 18^\circ$ with a gain variation less than 0.8 dBi. A detailed parametric analysis of the proposed unit cell is given to provide insights on how to achieve other beam steering angles for different applications.

The rest of this paper is organized as follows. The design of the unit cell is described in Section II. The whole antenna design is given in Section III as well as a comparison between the theoretical and experimental results. In Section IV, a current analysis by phased array theory for the proposed cell is illustrated. A discussion on the parametric effects is made in Section V. Finally, conclusions are drawn in Section VI.

II. DESIGN OF THE PRS UNIT CELL

This section presents the design of the proposed PRS unit cell. The schematic of the proposed unit cell is shown in Fig. 1. It consists of two back-to-back T-shaped strips with one PIN diode inserted in the center, and two symmetric trapezoid patches on both sides. The trapezoid patch in each side is constituted by a rectangular patch with a size of $l_2 \times w_2$ and a pair of triangle parasitic patches with dimensions of $w_2 = 8$ mm, $w_s = 0.5$ mm as shown in Fig. 1. The periodicity of this unit (P) is 20 mm ($0.37\lambda_0$). Other dimensions are listed in Table I. It should be pointed out that the T-shaped strips in each unit cell is connected with adjacent ones, which will simplify the biasing network.

The proposed unit is simulated using a periodic boundary condition in CST. Based on the PIN diode datasheet [23], the diode is modeled as a 2.1Ω resistor for ON-state and a parallel circuit consisting of a capacitor of 0.17 pF and a resistor of 3 k Ω for OFF-state. Its relevant model is

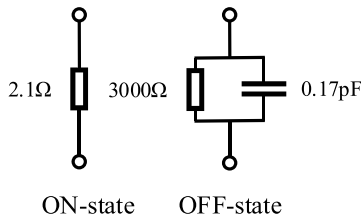


FIGURE 2. Model of the PIN diode in the simulation.

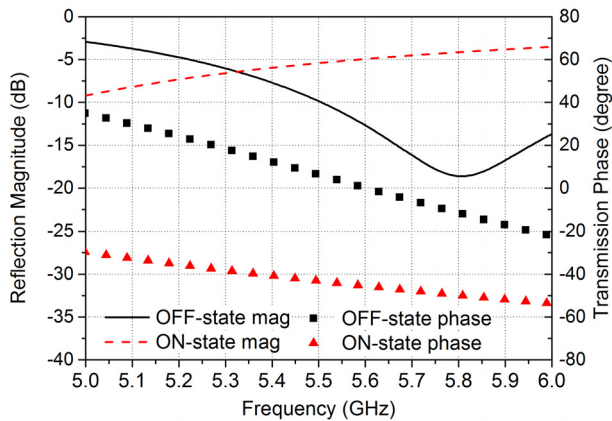


FIGURE 3. Simulated reflection/transmission coefficients of the proposed unit.

shown in Fig. 2. Fig. 3 shows the reflection magnitude and the transmission phase of the proposed unit cell. It can be seen that the phase difference between OFF and ON states is 49.4° at 5.5 GHz. The reflection magnitudes for OFF and ON states are -9.9 dB (reflectivity of 0.32) and -5.4 dB (reflectivity of 0.54), respectively. The reflectivity difference is only 0.22, which ensures that the gain variation is a small value. By employing 6×6 cells on the PRS, the beam is steered $\pm 18^\circ$ with respect to the broadside direction. Its detailed PRS performances and operating principle are given in the next section.

III. ANTENNA DESIGN AND RESULTS

Based on the above results, a PRS antenna with the proposed unit cells has been designed, fabricated, and measured. The schematics of the proposed PRS antenna are shown in Fig. 4. The dimensions of the antenna are $150 \text{ mm} \times 150 \text{ mm}$ ($2.75\lambda_0 \times 2.75\lambda_0$). It is fed by a microstrip square patch with a length of 13.2 mm ($0.24\lambda_0$). The patch antenna is etched on a 1.524-mm-thick Rogers 4003C substrate ($\epsilon_r = 3.55$, $\tan\delta = 0.0027$). The reconfigurable PRS structure and its biasing network are shown in Fig. 4 (b), which consists of 6×6 unit cells printed on the lower side of a 1.6-mm-thick FR4 substrate ($\epsilon_r = 4.4$, $\tan\delta = 0.018$).

The PRS is divided into two parts according to the group strategy. Each part consists of 3×6 cells. The cell sizes are the same as described in Section II. All the PIN diodes are oriented in the same direction. Since all the unit cells are connected, three PIN diodes on each row of each half of the PRS are connected in parallel. The six rows of PIN diodes

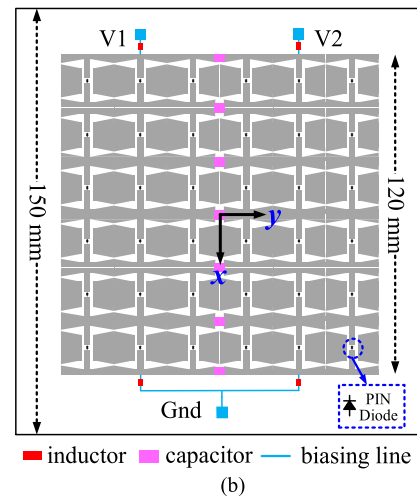
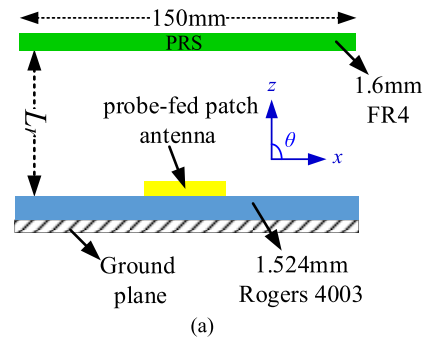


FIGURE 4. Schematic of (a) the whole antenna structure (side view) and (b) reconfigurable PRS structure with biasing lines.

on each half of the PRS are connected in series. As a result, the large number of inductors and biasing lines between adjacent cells in [17] are not needed. To independently control the two parts, seven capacitors are inserted along the middle line of the PRS for providing dc signal isolation. Therefore, the biasing network can be simplified as a combination of four inductors for RF choke and seven capacitors.

To calculate the cavity height of the proposed PRS antenna, the resonance condition below should be satisfied [3]

$$L_r = \left(\frac{\varphi}{\pi} - 1\right) \frac{\lambda}{4} + N \frac{\lambda}{2}, \quad N = 0, 1, 2, \dots \quad (1)$$

where φ is the reflection phase of the PRS. In this design, φ is decreased from -123.4° to -138.7° in the frequency range of 5-6 GHz and is chosen as -131° at 5.5 GHz for ON-state as an initial value. To achieve a better impedance matching, L_r is chosen as 32 mm by parametric study.

A photograph of the proposed PRS antenna is shown in Fig. 5. The proposed antenna has four states in total: All diodes turned OFF is named as State 1; All diodes turned ON is named as State 2; Diodes on the left group ON with the other OFF is named as State 3; Diodes on the right group OFF with the other ON is named as State 4.

The input reflection coefficients of the antenna were measured using an E5063A Agilent network analyzer. The radiation patterns and the realized gains were measured by using a nearfield antenna measurement system located

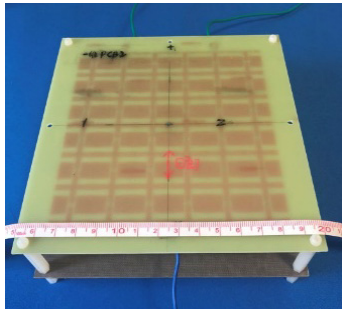


FIGURE 5. A photograph of the proposed PRS antenna.

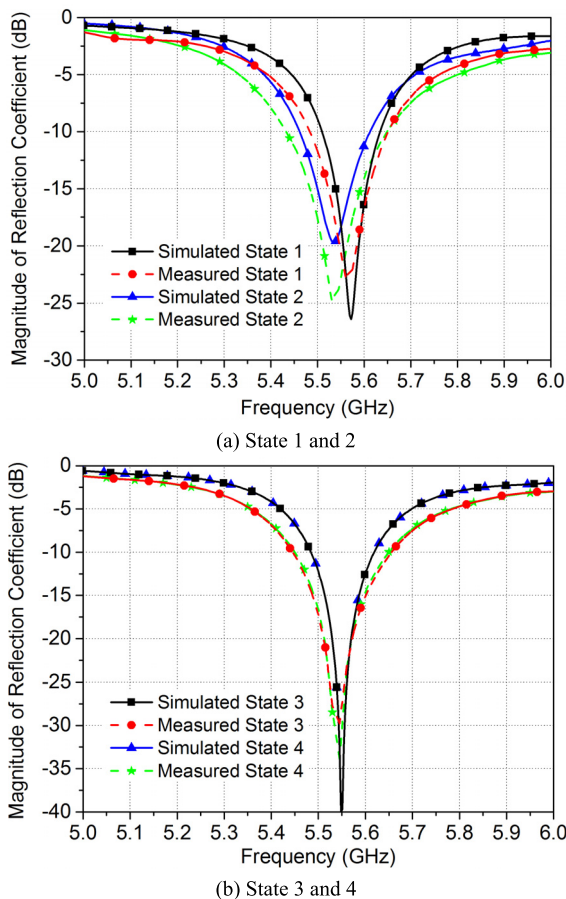


FIGURE 6. Magnitude of input reflection coefficient of the proposed antenna.

in Northwestern Polytechnical University. A WR187 open-ended rectangular waveguide probe was used as the transmitting antenna. Fig. 6 plots the predicted simulation and measurement input reflection coefficients for the four states. The measured results show that an overlapped impedance bandwidth of 5.45-5.65 GHz is achieved and that they agree well with the predicted simulation results.

Since the reflection magnitude for OFF-state is lower than ON-state as shown in Fig. 3, the gains of State 1 are much lower than the other three states. Hence, its pattern results are omitted here for brevity. The radiation patterns in the H-plane (yoz plane) for the three states are shown in Fig. 7.

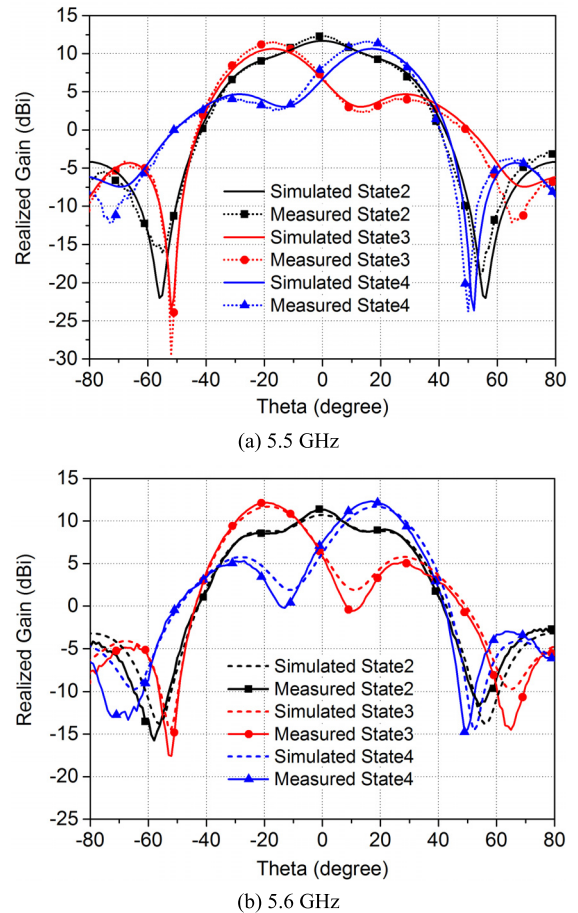


FIGURE 7. Realized gain patterns of the proposed antenna in the H-plane.

The predicted simulation and measurement results are seen to be in good agreement with each other. It is observed that a broadside radiation is obtained at State 2. For State 3 and State 4, the beam directions are tilted toward -18° and 18° from the broadside, respectively.

The realized gains are also given in Fig. 7. For State 2, the predicted simulation realized gains are 11.7 dBi and 10.7 dBi for 5.5 and 5.6 GHz, while the measured ones are 12.3 dBi and 11.4 dBi. For State 3 and State 4, the predicted simulation results are from 10.7 to 11.2 dBi, while the measured ones vary from 11.5 to 11.8 dBi. The maximum gain difference between State 3 and State 4 is 0.1 dBi, ensuring the symmetry of the beam steering property. For all states, the maximum gains exceed 11 dBi. Furthermore, the gain drops from the broadside direction to the tilted direction are 0.8 dBi and 0.5 dBi for 5.5 GHz and 5.6 GHz, respectively. The difference between the predicted simulation and measurement results is less than 1 dB for the three states.

IV. CURRENT ANALYSIS

To illustrate how the phase difference are generated, the current distributions of the unit cells are simulated in CST. We chose our previously designed unit cell in this section to show the potential of this proposed unit cell on how to realize a wide beam steering angle. Unit I refers to a patch-type unit

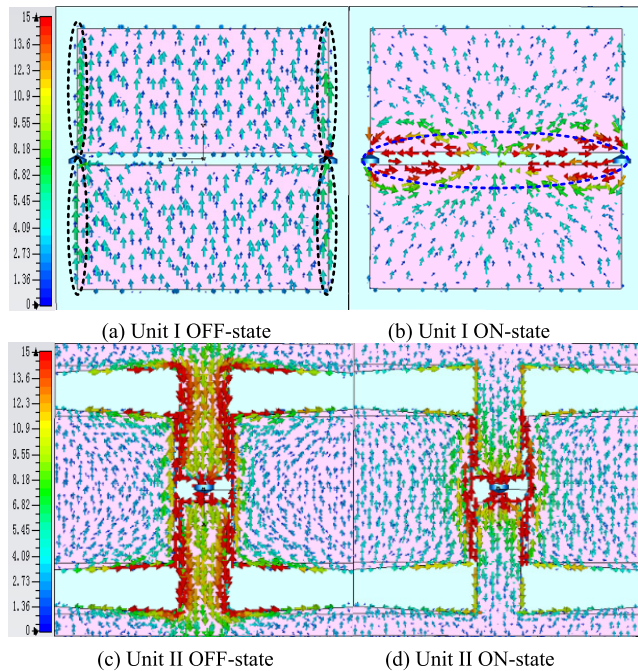


FIGURE 8. Simulated current distributions of Unit I/II.

cell with two PIN diodes inserted in the middle given in [17], as shown in Fig. 8 (a). Unit II is the proposed unit cell.

Fig. 8 plots the current distributions for different unit cells. As can be seen from Figs. 8 (a) and (b), the currents of Unit I are mainly distributed along the vertical edges (marked in black dotted circles) for OFF-state, while for ON-state the currents are concentrated along the center gap (marked in blue dotted circle). A small phase difference of 27.5° is produced due to the different lengths of the current path.

In order to enlarge the phase difference, Unit II is proposed, which can add more degrees of freedom to manipulate the current distribution. Figs. 8 (c) and (d) give the current distributions of Unit II. As is shown in Figs. 8 (c) and (d), the currents are concentrated along the T-shaped strips for both states. However, for OFF-state, the current path is much longer than that of ON-state. Therefore, a 49.4° phase difference between OFF-state and ON-state is achieved, which is much larger than that of Unit I.

Table II gives a performance comparison between Unit I and Unit II. Some predicted simulation results of their relevant PRS antennas are also given. Compared with Unit I, Unit II can realize a much larger beam steering angle with much fewer active elements. Therefore, it is a more attractive candidate cell for the PRS antennas in the applications of large beam steering angles, stable steering gains, and simple biasing networks.

V. DISCUSSION

As discussed in the previous sections, the beam steering angle increases with the phase difference between the two parts of the PRS with different PIN diodes states. There are many parameters of the proposed unit cell that affect the transmission phase. This section describes the parametric

TABLE 2. Simulated performance comparison among Unit I/II.

Performance	Unit	PRS antenna			
	Phase difference	Beam tilt angle	Max gain when tilting	Gain drop	Active/lumped elements No.
Unit I	27.5°	$\pm 5^\circ$	14.3 dBi	2.5 dBi	72+52
Unit II	49.4°	$\pm 18^\circ$	10.7 dBi	0.8 dBi	36+11

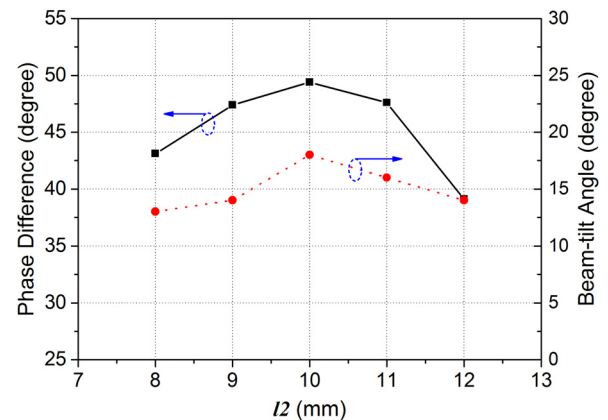


FIGURE 9. The effect of l_2 on unit phase difference and beam-tilt angle.

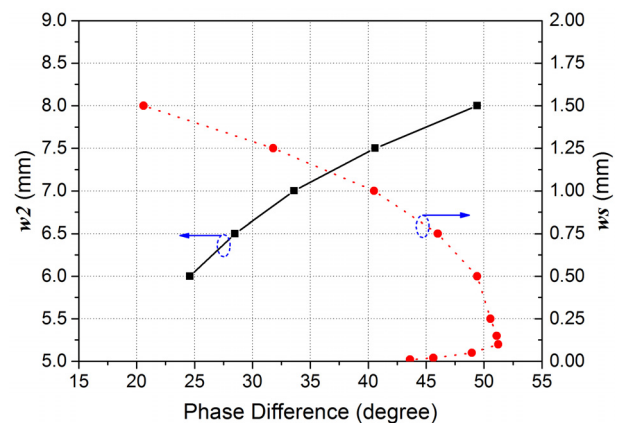


FIGURE 10. The effects of w_2 and w_s on unit phase difference.

study of some key parameters in order to show how we can realize different beam steering angles with the proposed PRS unit. When one parameter is changed, the others remain stable.

Fig. 9 shows the effects of the rectangular patch length l_2 on the phase difference of the unit and beam-tilt angle of the whole PRS antenna. It is seen that when l_2 is increased from 8 mm to 12 mm, the curve rises to its highest point at 10 mm then goes down. The phase difference variation range is from 39.1° ($l_2 = 12\text{mm}$) to 49.4° ($l_2 = 10\text{mm}$). Accordingly, the beam steering angle has a similar trend with a maximum value of 18° .

The effects of rectangular patch width w_2 and parasitic patch width w_s are investigated and given in Fig. 10.

TABLE 3. Comparison between the proposed antenna and reported antennas.

Antenna model	1-D Beam-tilt range	Size	Realized Gain	Gain drop	Unit No.	Tunable element No.
Antenna in [15]	$0, \pm 7^\circ$	$1.9 \lambda_0 \times 1.9 \lambda_0$	Directivity 14.8 dBi	NG	12 rows of grids	144+12 potentiometers
Antenna in [16]	$0, \pm 28^\circ$	$5.7 \lambda_0 \times 5.7 \lambda_0$	NG	NG	30×30	600
Antenna in [17]	$0, \pm 5^\circ$	$3.1 \lambda_0 \times 3.1 \lambda_0$	11.8–14.3 dBi	2.5 dBi	6×6	72+52
Antenna in this paper	$0, \pm 18^\circ$	$2.75 \lambda_0 \times 2.75 \lambda_0$	11.5–12.3 dBi	0.8 dBi	6×6	36+11

w_2 and w_3 have much more prominent influences than l_2 , which can lead to a phase change range from 20° to 50° . However, they have opposite variation trends: The phase difference increases with w_2 , while it increases when w_3 decreases. It is noted that when w_3 decreases to 0.1, the phase difference reaches its maximum value. The phase difference decreases when w_3 is smaller than 0.1 since the size of triangle parasitic patch is rather small and no currents will be induced by this parasitic structure. For achieving a larger phase difference with a small fabrication error, $w_2 = 8\text{mm}$ and $w_3 = 0.5\text{mm}$ are chosen in this design.

A comparison of the radiation performance, antenna size, and tunable element number of the proposed PRS antenna with some reported designs are described in Table III. As can be seen from the table, the proposed antenna has a larger beam steering angle with a smaller gain variation range and much fewer tunable elements employed.

VI. CONCLUSION

In order to enhance the beam steering capability for PRS antennas while maintaining a simple network with fewer active/lumped elements, a novel reconfigurable unit cell has been proposed and investigated in this paper. By employing 6×6 such unit cells on the PRS, the proposed antenna can achieve a $\pm 18^\circ$ electronic beam steering with respect to the broadside direction, across an overlapped 10-dB impedance bandwidth of 5.45–5.65 GHz. The measured realized gains are over 11 dBi for all states with a maximum gain drop less than 0.8 dBi. Compared with other reported beam steering designs, the proposed antenna has the advantages of a rather small gain drop and a much simpler biasing network with a stable beam-tilt performance.

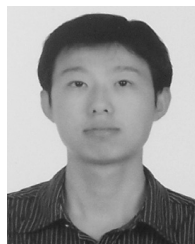
ACKNOWLEDGMENT

The authors thank Prof. Wei Feng for assisting with the measurement of the biasing network.

REFERENCES

- [1] L. Leger, T. Monediere, and B. Jecko, "Enhancement of gain and radiation bandwidth for a planar 1-D EBG antenna," *IEEE Microw. Wireless Compon. Lett.*, vol. 15, no. 9, pp. 573–575, Sep. 2005.
- [2] R. Gardelli, M. Albani, and F. Capolino, "Array thinning by using antennas in a Fabry–Perot cavity for gain enhancement," *IEEE Trans. Antennas Propag.*, vol. 54, no. 7, pp. 1979–1990, Jul. 2006.
- [3] G. V. Trentini, "Partially reflecting sheet arrays," *IRE Trans. Antennas Propag.*, vol. 4, no. 4, pp. 666–671, Oct. 1956.
- [4] Z. Liu, W. Zhang, D. Fu, Y. Gu, and Z. Ge, "Broadband Fabry–Perot resonator printed antennas using FSS superstrate with dissimilar size," *Microw. Opt. Technol. Lett.*, vol. 50, no. 6, pp. 1623–1627, Jun. 2008.
- [5] Y. Ge, K. P. Esselle, and T. S. Bird, "The use of simple thin partially reflective surfaces with positive reflection phase gradients to design wideband, low-profile EBG resonator antennas," *IEEE Trans. Antennas Propag.*, vol. 62, no. 2, pp. 743–750, Feb. 2012.
- [6] N. Wang, J. Li, G. Wei, L. Talbi, Q. Zeng, and J. Xu, "Wideband Fabry–Perot resonator antenna with two layers of dielectric superstrates," *IEEE Antennas Wireless Propag. Lett.*, vol. 14, pp. 229–232, 2015.
- [7] F. Wu and K. M. Luk, "Wideband high-gain open resonator antenna using a spherically modified, second-order cavity," *IEEE Trans. Antennas Propag.*, vol. 65, no. 4, pp. 2112–2116, Apr. 2017.
- [8] L.-Y. Ji, P.-Y. Qin, and Y. J. Guo, "Wideband Fabry–Perot cavity antenna with a shaped ground plane," *IEEE Access*, vol. 6, pp. 2291–2297, 2017.
- [9] D. Parker and D. C. Zimmermann, "Phased arrays—Part 1: Theory and architectures," *IEEE Trans. Microw. Theory Techn.*, vol. 50, no. 3, pp. 678–687, Mar. 2002.
- [10] Y.-Y. Bai, S. Xiao, M.-C. Tang, Z.-F. Ding, and B.-Z. Wang, "Wide-angle scanning phased array with pattern reconfigurable elements," *IEEE Trans. Antennas Propag.*, vol. 59, no. 11, pp. 4071–4076, Nov. 2011.
- [11] C. Ding, Y. J. Guo, P.-Y. Qin, and Y. Yang, "A compact microstrip phase shifter employing reconfigurable defected microstrip structure (RDMS) for phased array antennas," *IEEE Trans. Antennas Propag.*, vol. 63, no. 5, pp. 1985–1996, May 2015.
- [12] A. Ghasemi, S. N. Burokur, A. Dhoubi, and A. de Lustrac, "High beam steering in Fabry–Pérot leaky-wave antennas," *IEEE Antennas Wireless Propag. Lett.*, vol. 12, pp. 261–264, 2013.
- [13] B. Ratni, W. A. Merzouk, A. de Lustrac, S. Villers, G.-P. Piau, and S. N. Burokur, "Design of phase-modulated metasurfaces for beam steering in Fabry–Perot cavity antennas," *IEEE Antennas Wireless Propag. Lett.*, vol. 16, pp. 1401–1404, 2016.
- [14] S. N. Burokur, J.-P. Daniel, P. Ratajczak, and A. de Lustrac, "Tunable bilayered metasurface for frequency reconfigurable directive emissions," *Appl. Phys. Lett.*, vol. 97, no. 6, Aug. 2010, Art. no. 064101.
- [15] A. Ourir, S. N. Burokur, and A. de Lustrac, "Electronic beam steering of an active metamaterial-based directive subwavelength cavity," in *Proc. 2nd Eur. Conf. Antennas Propag.*, Edinburgh, U.K., Nov. 2007, pp. 1–4.
- [16] B. Ratni, A. de Lustrac, G.-P. Piau, and S. N. Burokur, "Modeling and design of metasurfaces for beam scanning," *Appl. Phys. A, Solids Surf.*, vol. 123, p. 50, Jan. 2017.
- [17] L.-Y. Ji, Y. J. Guo, P.-Y. Qin, S.-X. Gong, and R. Mitra, "A reconfigurable partially reflective surface (PRS) antenna for beam steering," *IEEE Trans. Antennas Propag.*, vol. 63, no. 6, pp. 2387–2395, Jun. 2015.

- [18] R. Guzman-Quiros, J. L. Gomez-Tornero, A. R. Weily, and Y. J. Guo, "Electronically steerable 1-D Fabry-Pérot leaky-wave antenna employing a tunable high impedance surface," *IEEE Trans. Antenna Propag.*, vol. 60, no. 11, pp. 5046–5055, Nov. 2012.
- [19] R. Guzman-Quiros, J. L. Gomez-Tornero, A. R. Weily, and Y. J. Guo, "Electronic full-space scanning with 1-D Fabry-Pérot LWA using electromagnetic band-gap," *IEEE Antennas Wireless Propag. Lett.*, vol. 11, pp. 1426–1429, 2012.
- [20] R. Guzman-Quiros, A. R. Weily, J. L. Gomez-Tornero, and Y. J. Guo, "A Fabry-Pérot antenna with two-dimensional electronic beam scanning," *IEEE Trans. Antennas Propag.*, vol. 64, no. 4, pp. 1536–1541, Apr. 2016.
- [21] P. Xie, G. Wang, H. Li, and J. Liang, "A dual-polarized two-dimensional beam-steering Fabry-Pérot cavity antenna with a reconfigurable partially reflecting surface," *IEEE Antennas Wireless Propag. Lett.*, vol. 16, pp. 2370–2374, 2017.
- [22] L.-Y. Ji, Z.-Y. Zhang, and N.-W. Liu, "A two-dimensional beam-steering partially reflective surface (PRS) antenna using a reconfigurable FSS structure," *IEEE Antennas Wireless Propag. Lett.*, vol. 18, no. 6, pp. 1076–1080, Jun. 2019.
- [23] *Infineon Datasheet for Bar64-02V*. Accessed: Feb. 14, 2003. [Online]. Available: <https://www.alldatasheet.com/datasheet-pdf/pdf/78978/infineon/bar64-02v.html>



PEI-YUAN QIN (M'13) was born in Liaoning, China, in 1983. He received the bachelor's degree in electronic engineering from Xidian University, Xi'an, China, in 2006, and the joint Ph.D. degree in electromagnetic fields and microwave technology from Xidian University and Macquarie University, Australia, in 2012.

He is currently a Senior Lecturer with UTS. His research interests include reconfigurable antennas, phase shifters, reconfigurable reflect arrays, and MIMO communications.



JIAN-YING LI received the Ph.D. degree in electromagnetics from Xidian University, in 1992.

From 2001 to 2010, he was a Research Scientist with the National University of Singapore. He is currently a Professor with Northwestern Polytechnical University. His research interests include electrically small antenna, wideband antenna arrays, and conformal antenna arrays.



LU-YANG JI was born in Shaanxi, China, in 1989. She received the B.S. degree in electronic engineering and the Ph.D. degree in electromagnetics from Xidian University, in 2010 and 2016, respectively.

From 2013 to 2015, she was a Visiting Ph.D. Student in reconfigurable antennas with CSIRO DPAS Flagship, Marsfield, Australia. She is currently an Assistant Professor with Northwestern Polytechnical University. Her research interests include reconfigurable antennas and wideband antennas.



LIN-XI ZHANG received the B.S. degree in electronic engineering from the Nanjing University of Science and Technology, in 1986, and the M.S. degree in communication and electronic system from the Beijing Institute of Technology, in 1991.

He is the Deputy Director with the Radio laboratory, Unmanned Aerial Vehicle Research Institute, Northwestern Polytechnical University. He is currently a Professor with Northwestern Polytechnical University. His research interests include RCS reduction of the unmanned systems and antenna measurements.

• • •